

# Deep Adversarial Attention Alignment for Unsupervised Domain Adaptation: the Benefit of Target Expectation Maximization

Guoliang Kang, Liang Zheng, Yan Yan, Yi Yang  
Center for Artificial Intelligence  
University of Technology Sydney

Guoliang.Kang@student.uts.edu.au, liangzheng06@gmail.com,  
{yan.yan-3@student, yi.yang}@uts.edu.au

## Abstract

In this paper we make two contributions to unsupervised domain adaptation in the convolutional neural network. First, our approach transfers knowledge in the deep side of neural networks for all convolutional layers. Previous methods usually do so by directly aligning higher-level representations, e.g., aligning the activations of fully-connected layers. In this case, although the convolutional layers can be modified through gradient back-propagation, but not significantly. Our approach takes advantage of the natural image correspondence built by CycleGAN. Departing from previous methods, we use every convolutional layer of the target network to uncover the knowledge shared by the source domain through an attention alignment mechanism. The discriminative part of an image is relatively insensitive to the change of image style, ensuring our attention alignment particularly suitable for robust knowledge adaptation. Second, we estimate the posterior label distribution of the unlabeled data to train the target network. Previous methods, which iteratively update the pseudo labels by the target network and refine the target network by the updated pseudo labels, are straightforward but vulnerable to noisy labels. Instead, our approach uses category distribution to calculate the cross-entropy loss for training, thereby ameliorating deviation accumulation. The two contributions make our approach outperform the state-of-the-art methods by +2.6% in all the six transfer tasks on Office-31 on average. Notably, our approach yields +5.1% improvement for the challenging  $\mathbf{D} \rightarrow \mathbf{A}$  task.

## 1. Introduction

This paper focuses on unsupervised domain adaptation. This task aims to adapt the knowledge from a source network, trained by the source domain data, to facilitate the training of a target network, which will be used for testing

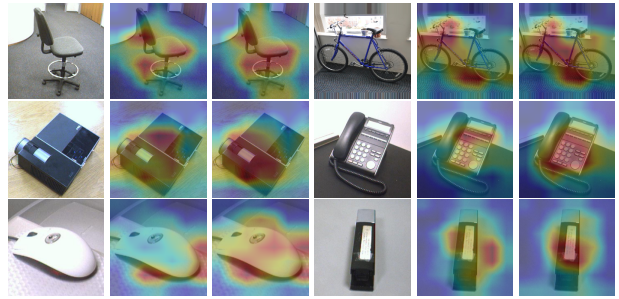


Figure 1: Visualization of attention exhibited by CNNs fine-tuned on source and target domain (assume being labeled), respectively, for target images. By comparison, CNN trained on the target domain pays more attention to the discriminative parts of the objects, while CNN trained on the source domain focuses more on the irrelevant background. This paper thus intends to perform attention alignment during domain adaptation. In each triplet, **Left**: a target image, **Middle**: attention produced by CNN fine-tuned on the source domain, **Right**: attention produced by CNN fine-tuned on the target domain.

in the target domain. Note that in this task the *target domain is unlabeled*. The increasing popularity of this task is because the performance of the model well-fitted to one domain may degenerate heavily on another one if the underlying data distributions across domains vary a lot.

In essence, the attention mechanism is emphasized as a key ingredient for CNN, suggested by a number of studies [22, 28, 30, 20, 27]. Zagoruyko *et al.* [27] find that the model performance is highly correlated with the attention mechanism: a stronger model always owns better aligned attention than a weaker one. This paper, partially motivated by [27], aims to align the attention of a source network and a target network to input images with the same underlying content. In fact, from Fig. 1, given an image from domain

$A$ , suppose we have a model trained on domain  $A$  and a model trained on domain  $B$ . When we visualize the attention of two models on this image, we observe distinct attention distributions on the image. This phenomenon indicates that the two models are poorly aligned in terms of the attention mechanism. The fact that domain shift deteriorates the attention mechanism may exert negative influence on the classification system. Therefore, this paper expects that the attention of a network should be *invariant to domain shift*.

In the community of unsupervised domain adaptation, many deep learning methods attempt to minimize the discrepancy between domains on the top layers, such as the fully connected layers, of the neural network via explicitly imposing penalty terms [26, 13, 14, 23] or in an adversarial way [5, 25, 24]. While the modifications at the fully connected layers can be back-propagated in principle, it may decay after a few layers, especially when gradient explosion or vanishing takes place. Consequently, the convolutional layer may be under-constrained and cannot be well adapted to the target domain. So it remains unknown how to constrain the behavior of convolutional layers to enable them better adapted to the target domain data.

Based on the above discussions, this paper proposes to align the attention of the target network with that of the source network. Our assumption is that no matter how domain varies, the discriminative parts of an image are insensitive to the changes of image style. In this procedure, the main obstacle to perform attention alignment is the lack of data correspondence. We propose using CycleGAN [31] to translate the data from one domain to another without modifying its underlying content. Then, for the paired samples (*e.g.* real source (or target) image and synthetic target (or source) image), we explicitly penalize the distances between attention maps of the source and the target models.

Additionally, we train our target network with real and synthetic data from both source and target domains. For source domain and its translated data, we impose the cross-entropy loss between the predictions and the ground-truth labels. For target domain and its translated source domain data, due to the lack of ground-truth labels, we make use of their underlying category distributions which provide insight into the target data. In a nutshell, we adopt the modified Expectation Maximization (EM) steps to maximize the likelihood of target domain images and update the model. Training iterations improve both the label posterior distribution estimation and the discriminative ability of the model.

Our contributions are summarized below,

- We propose a deep attention alignment method which allows the target network to mimic the attention of the source network. Taking advantage of the pairing nature of CycleGAN, no additional supervision is needed.
- We propose using EM algorithm to exploit the unlabeled target data to update the network. Several modifications are made to stabilize training and improve the adaptation performance.
- Our method outperforms the state of art in all the six transfer tasks, achieving +2.6% improvement in average on the real-world domain adaptation dataset Office-31.

## 2. Related Work

**Unsupervised domain adaptation.** Various methods have been proposed for unsupervised domain adaptation [26, 13, 5, 16, 17, 14]. Many works try to make the representations at the tail of neural networks invariant across domains. Tzeng *et al.* [26] propose a kind of domain confusion loss to encourage the network to learn both semantically meaningful and domain invariant representations. Similarly, Long *et al.* [13] minimize the MMD distance of the fully-connected activations between source and target domain while sharing the convolutional features. Ganin *et al.* [5] enable the network to learn domain invariant representations in an adversarial way by adding a domain classifier and back-propagating inverse gradients. JAN [14] penalizes the joint MMD over multiple fully-connected layers to minimize the domain discrepancy coming from both the data distribution and the label distribution. Few works pay attention to the domain shift coming from the convolutional layers. In this paper, we notice that the attention mechanism cannot be preserved when directly applying the model trained on the source domain to the target domain. To alleviate this problem, we constrain the training of convolutional layers by imposing the attention alignment penalty across domains.

**Attention of CNNs.** The study of the attention mechanism of computational models is inspired by human vision experience that human tends to focus their attention on the object of interest. Nowadays, attention is widely adopted in various applications, *e.g.*, object recognition, visual captioning, and NLP. Here we focus on works *w.r.t* understanding and representing visual attention mechanisms of CNNs.

There exist many ways to define and visualize the attention mechanisms learned by CNNs. Zeiler & Fergus [28] project certain features back onto the image through a network called “deconvnet” which shares the same weights as the original feed-forward network. Simonyan *et al.* [22] propose using the gradient of the class score *w.r.t* the input image to visualize the CNN. Class activation maps (CAMs), proposed by [30], aim to visualize the class-discriminative image regions used by a CNN. Grad-CAM [20] combines gradient based attention method and CAM, enabling to obtain class-discriminative attention maps without modifying the original network structure as [30].

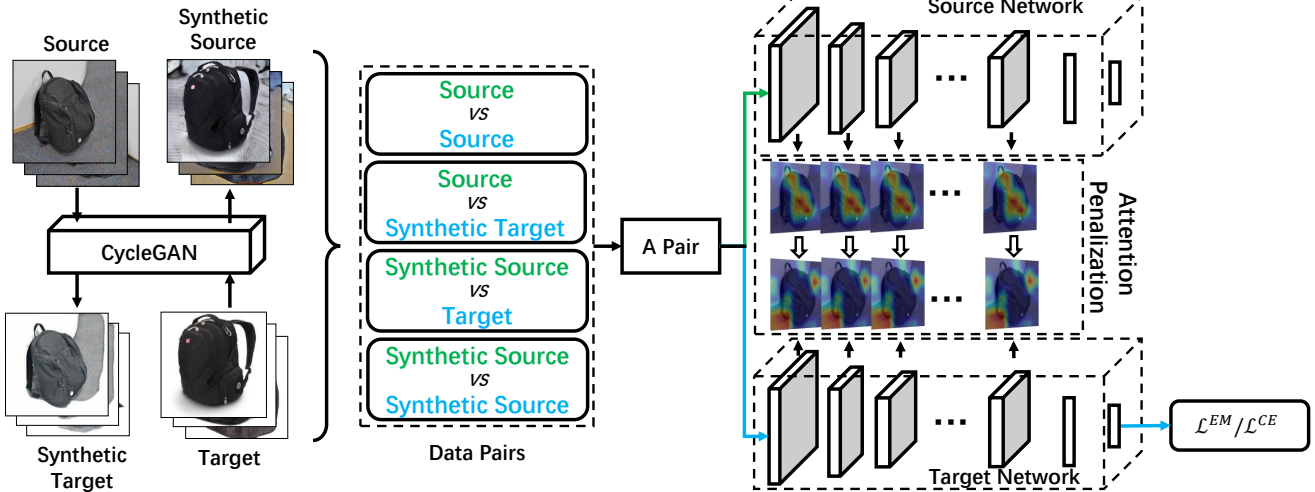


Figure 2: The framework of deep adversarial attention alignment. We train a source network and fix it. The source network guides the attention alignment of the target network. The target network is trained with real source and synthetic target images from both domains. For labeled real source and synthetic target data, we update the network by computing the cross-entropy loss between the predictions and the ground-truth labels. For unlabeled real target and synthetic source images, we maximize the likelihood of the data with EM steps. The attention distance for a pair of images (as illustrated in the “Data Pairs” block) passing through the source network and the target network, respectively, is minimized.

Zagoruyko *et al.* [27] define attention as a set of spatial maps indicating which area the network focuses on to perform a certain task. The attention maps can also be defined *w.r.t* various layers of the network so that they are able to capture both low-, mid-, and high-level representation information. They propose that attention mechanism should be a kind of knowledge transferred across different *network architectures*. Zaogruyko *et al.* [27] align the attention across different architectures for exactly the same image during the training process and aim to transfer the knowledge from a large model to a smaller one. Different to [27], our method aligns the attention across different *data domains* where images across domains are unpaired and aims to promote the model adaptation performance across domains.

**Unpaired image-to-image translation.** Unpaired image-to-image translation aims to train a model to map image samples across domains, under the absence of pairing information. It can be realized through GAN to pair the real source (or target) and synthetic target (or source) images [12, 21, 31, 9, 11, 2, 8, 18]. Generating synthetic images can be beneficial for various vision tasks [15, 29]. In this paper, we concentrate on maximizing the utility of given paired real and synthetic samples. And we choose CycleGAN [31] to perform such adversarial data pairing. A better GAN framework will promote the performance of our method, however the discussions of which exceed the scope of this paper.

### 3. Deep Adversarial Attention Alignment

Our framework is illustrated in Fig. 2. We train a source CNN which guides the attention alignment of the target CNN whose convolutional layers have the same architecture as the source network. The target CNN is trained with a mixture of real and synthetic images from both source and target domains. For source and synthetic target domain data, we have ground-truth labels and use them to train the target network with cross-entropy loss. On the other hand, for the target and synthetic source domain data, due to the lack of ground-truth labels, we optimize the target network through an EM algorithm.

#### 3.1. Adversarial Data Pairing

We use CycleGAN to translate the samples in the source domain  $S$  to those in the target domain  $T$ , and vice versa. The underlying assumption to obtain meaningful translation is that there exist some relationships between two domains. For unsupervised domain adaptation, the objects of interest across domains belong to the same set of category. So it is possible to use CycleGAN to map the sample in the source domain to that in the target domain while maintaining the underlying object-of-interest.

The Generative Adversarial Network (GAN) aims to generate synthetic images which are indistinguishable from

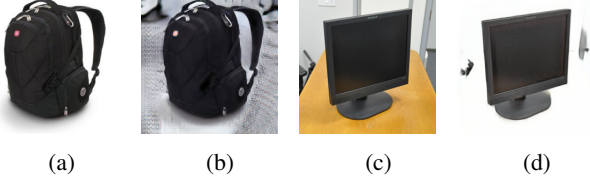


Figure 3: Pairing data across domains using CycleGAN. (a) and (c): real images sampled from source and target domain, respectively. (b): a synthetic target image paired with (a) through  $G^{ST}$ . (d): a synthetic source image paired with a real target image (c) through  $G^{TS}$ .

real samples through an adversarial loss,

$$\begin{aligned} \mathcal{L}^{GAN}(G^{ST}, D^T, X^S, X^T) = & \mathbb{E}_{x^T}[\log D^T(x^T)] \\ & + \mathbb{E}_{x^S}[1 - \log D^T(G^{ST}(x^S))], \end{aligned} \quad (1)$$

where  $x^S$  and  $x^T$  are sampled from source domain  $S$  and target domain  $T$ , respectively. The generator  $G^{ST}$  mapping  $X^S$  to  $X^T$  strives to make its generated synthetic outputs  $G^{ST}(x^S)$  indistinguishable from real target samples  $x^T$  for the domain discriminator  $D^T$ .

Because the training data across domains are unpaired, the translation from source domain to target domain is highly under-constrained. CycleGAN couples the adversarial training of this mapping with its inverse one, *i.e.* the mapping from  $S$  to  $T$  and that from  $T$  to  $S$  are learned concurrently. Moreover, it introduces a cycle consistency loss to regularize training,

$$\begin{aligned} \mathcal{L}^{cyc}(G^{ST}, G^{TS}) = & \mathbb{E}_{x^S}[\|G^{TS}(G^{ST}(x^S)) - x^S\|_1] \\ & + \mathbb{E}_{x^T}[\|G^{ST}(G^{TS}(x^T)) - x^T\|_1], \end{aligned} \quad (2)$$

Formally, the full objective for CycleGAN is,

$$\begin{aligned} \mathcal{L}^{cyc}(G, F, D_X, D_Y) = & \mathcal{L}^{GAN}(G^{ST}, D^T, X^S, X^T) \\ & + \mathcal{L}^{GAN}(G^{TS}, D^S, X^T, X^S) \\ & + \lambda \mathcal{L}^{cyc}(G^{ST}, G^{TS}), \end{aligned} \quad (3)$$

where the constant  $\lambda$  controls the strength of the cycle consistency loss. Through CycleGAN, we are able to translate an image in the source domain to that in the target domain in the context of our visual domain adaptation tasks, as illustrated in Fig. 3.

As illustrated in Fig. 1, the target model pays too much attention to the irrelevant background or less discriminative parts of the objects of interest. This attention misalignment will degenerate the model’s performance. In this paper, we propose to use the style-translated images as natural image correspondences to guide the attention mechanism of the target model to mimic that of the source model, to be detailed in Section 3.2.

### 3.2. Attention Alignment

Based on the paired images, we propose imposing the attention alignment penalty to reduce the discrepancy of attention maps across domains. Specifically, we represent attention as a function of spatial maps *w.r.t* each convolutional layer [27]. For the input  $x$  of a CNN, let the corresponding feature maps *w.r.t* layer  $l$  be represented by  $F_l(x)$ . Then, the attention map  $A_l(x)$  *w.r.t* layer  $l$  is defined as

$$A_l(x) = \sum_c |F_{l,c}(x)|^2, \quad (4)$$

where  $F_{l,c}(x)$  denotes the  $c$ -th channel of the feature maps. The operations in Eq. (4) are all element-wise. Alternative ways to represent the attention maps include  $\sum_c |F_{l,c}|$ , and  $\max |F_{l,c}|$ , *etc.* We adopt Eq. (4) to emphasize the salient parts of the feature maps.

We propose using the source network to guide the attention alignment of the target network, as illustrated in Fig. 2. We penalize the distance between the vectorized attention maps between the source and the target networks to minimize their discrepancy. In order to make the attention mechanism invariant to the domain shift, we train the target network with a mixture of real and synthetic data from both source and target domains.

Formally, the attention alignment penalty can be formulated as,

$$\begin{aligned} \mathcal{L}^{AT} = & \sum_l \left\{ \sum_i \left\| \frac{A_l^S(x_i^S)}{\|A_l^S(x_i^S)\|_2} - \frac{A_l^T(x_i^S)}{\|A_l^T(x_i^S)\|_2} \right\| \right. \\ & + \sum_j \left\| \frac{A_l^S(x_j^S)}{\|A_l^S(x_j^S)\|_2} - \frac{A_l^T(\tilde{x}_j^T)}{\|A_l^T(\tilde{x}_j^T)\|_2} \right\| \\ & + \sum_m \left\| \frac{A_l^S(\tilde{x}_m^S)}{\|A_l^S(\tilde{x}_m^S)\|_2} - \frac{A_l^T(\tilde{x}_m^S)}{\|A_l^T(\tilde{x}_m^S)\|_2} \right\| \\ & \left. + \sum_n \left\| \frac{A_l^S(\tilde{x}_n^S)}{\|A_l^S(\tilde{x}_n^S)\|_2} - \frac{A_l^T(x_n^T)}{\|A_l^T(x_n^T)\|_2} \right\| \right\}, \end{aligned} \quad (5)$$

where the subscript  $l$  denotes the layer and  $i, j$  denote the samples. The  $A_l^S$  and  $A_l^T$  represent the attention maps *w.r.t* layer  $l$  for the source network and the target network, respectively.  $x^S$  and  $x^T$  are real source and real target domain data, respectively. The synthetic target data  $\tilde{x}_i^T$  and synthetic source data  $\tilde{x}_n^S$  satisfy  $\tilde{x}_i^T = G^{ST}(x_i^S)$  and  $\tilde{x}_n^S = G^{TS}(x_n^T)$ , respectively.

Through Eq. (5), the distances of attention maps for the paired images (*i.e.*,  $(x_j^S, \tilde{x}_j^T)$  and  $(x_n^T, \tilde{x}_n^S)$ ) are minimized. Moreover, We additionally penalize the attention maps of the same input (*i.e.*,  $x_i^S$  and  $\tilde{x}_m^S$ ) passing through different networks. The attention alignment penalty  $\mathcal{L}^{AT}$  allows the attention mechanism to be gradually adapted to the target domain, which makes the attention mechanism of the target network invariant to domain shift.

**Remark.** Considering minimizing the discrepancy across domains, our method shares the same idea with DAN [13] and JAN [14]. The difference is that our method works on the convolutional layers where structural information is critical; in comparison, DAN or JAN works on the fully-connected layers where high-level semantic information is considered. Another notable difference is that our method deals with more refined sample-level discrepancy through adversarial data pairing, whereas DAN or JAN considers discrepancy from coarse distribution-level.

In DAN and JAN, MMD and JMMD criteria are adopted respectively to measure the distances of feature distributions across domains. As the distance measure, MMD or JMMD can be used to perform attention alignment technically, but not as effective because when integrated into our system, MMD or JMMD maps the attentions to the RKHS space so that the structure information is lost. The superiority of our method is confirmed in the experiment part by comparing different distance criteria for performing attention alignment.

### 3.3. Training with EM

To make full use of the available data (labeled and unlabeled), we train the target-domain model with a mixture of real and synthetic data from both source and target domains, as illustrated in Fig. 2. For the source and its translated synthetic target domain data, we compute the cross-entropy loss between the predictions and ground-truth labels to back-propagate the gradients through the target network. The cross-entropy loss for the source and corresponding synthetic target domain data can be formulated as follows,

$$\mathcal{L}^{CE} = -\left[\sum_i \log p_\theta(y_i^S | x_i^S) + \sum_j \log p_\theta(y_j^S | \tilde{x}_j^T)\right], \quad (6)$$

where  $y^S \in \{1, 2, \dots, K\}$  denotes the label for the source sample  $x^S$  and the translated synthetic target sample  $\tilde{x}^T$ . The probability  $p_\theta(y|x)$  is represented by the  $y$ -th output of the target network with parameters  $\theta$  given the input image  $x$ .  $\tilde{x}_j^T = G^{ST}(x_j^S)$ .

For the unlabeled target data, due to the lack of labels, we employ the EM algorithm to optimize the target network. The EM algorithm can be split into two alternative steps: the **(E)**xpectation computation step and the expectation **(M)**aximization step. The objective is to maximize the log-likelihood of target data samples,

$$\sum_i \log p_\theta(x_i^T), \quad (7)$$

In image classification, our prior is that the target data samples belong to  $K$  different categories. We choose the underlying category  $z_i \in \{1, 2, \dots, K\}$  of each sample as the

hidden variable, and the algorithm is depicted as follows (we omit the sample subscript and the target domain superscript for description simplicity).

**(i) The Expectation step.** We first estimate  $p_{\theta_{t-1}}(z|x)$  through,

$$p_{\theta_{t-1}}(z|x) = \frac{p_{\theta_{t-1}}(x|z)p(z)}{\sum_z p_{\theta_{t-1}}(x|z)p(z)}, \quad (8)$$

where the distribution  $p_{\theta_{t-1}}(z|x)$  is modeled by the target network.  $\theta_{t-1}$  is the parameters of the target-domain CNN at last training step  $t-1$ . We adopt the uniform distribution to depict  $p(z)$ , *i.e.*, assuming the occurrence probabilities of all the categories are the same. In this manner,  $p_{\theta_{t-1}}(z|x) = p_{\theta_{t-1}}(x|z)$  is satisfied.

**(ii) The Maximization step.** Based on the computed posterior  $p_{\theta_{t-1}}(z|x)$ , our objective is to update  $\theta_t$  to improve the lower bound of Eq. (7),

$$\sum_z p_{\theta_{t-1}}(z|x) \log p_{\theta_t}(x|z) \quad (9)$$

Note that we omit  $\sum_z p_{\theta_{t-1}}(z|x) \log p(z)$  because we assume  $p(z)$  subjects to the uniform distribution which is irrelevant to  $\theta_t$ . Also, because  $p_\theta(z|x) = p_\theta(x|z)$ , Eq. (9) is equivalent to,

$$\sum_z p_{\theta_{t-1}}(z|x) \log p_{\theta_t}(z|x). \quad (10)$$

Moreover, we propose to improve the effectiveness and stability of the above EM steps through three aspects

A) Asynchronous update of  $p(z|x)$ . We adopt an independent network  $M^{post}$  to estimate  $p(z|x)$  and update  $M^{post}$  asynchronously, *i.e.*,  $M^{post}$  synchronizes its parameters  $\theta^{post}$  with the target network every  $N$  steps:

$$\theta_t^{post} = \theta_{\lfloor t/N \rfloor \times N}. \quad (11)$$

In this manner, we avoid the frequent update of  $p(z|x)$  and make the training process much more stable.

B) Filtering the inaccurate estimates. Because the estimate of  $p(z|x)$  is not accurate, we set a threshold  $p_t$  and discard the samples whose maximum value of  $p(z|x)$  over  $z$  is lower than  $p_t$ .

C) Initializing the learning rate schedule after each update of  $M^{post}$ . To accelerate the target network adapting to the new update of the distribution  $p(z|x)$ , we choose to initialize the learning rate schedule after each update of  $M^{post}$ .

Note that for synthetic source data  $\tilde{x}^S = G^{TS}(x^T)$ , we can also applied the modified EM steps for training. Because  $G^{TS}$  is a definite mapping, we assume  $p(z|\tilde{x}^S) = p(z|x^T)$ .

To summarize, when using the EM algorithm to update the target network with target data and synthetic source

data, we first compute the posterior  $p(z|x^T)$  through network  $M^{post}$  which synchronizes with the target network every  $N$  steps. Then we minimize the loss,

$$\begin{aligned} \mathcal{L}^{EM} = & -\left\{ \sum_i \sum_{z_i} p_{\theta^{post}}(z_i|x_i^T) \log p_{\theta}(z_i|x_i^T) \right. \\ & \left. + \sum_j \sum_{z_j} p_{\theta^{post}}(z_j|x_j^T) \log p_{\theta}(z_j|\tilde{x}_j^S) \right\}. \end{aligned} \quad (12)$$

In our experiment, we show that these modifications yield consistent improvement over the basic EM algorithm.

### 3.4. Deep Adversarial Attention Alignment

Based on the above discussions, our full objective for training the target network can be formulated as,

$$\mathcal{L}^{full} = \mathcal{L}^{CE} + \mathcal{L}^{EM} + \beta \mathcal{L}^{AT} \quad (13)$$

where  $\beta$  determines the strength of the attention alignment penalty term  $\mathcal{L}^{AT}$ .

**Discussions.** The recipe for our approach consists of two parts: adversarial attention alignment and EM training. Adversarial attention alignment plays an important role in the success of our approach. On the one hand, adversarial data pairing provides natural image correspondences to perform attention alignment, while attention alignment built on such image correspondences reduces the system reliance on the quality of the synthetic images (*i.e.*, how close it is to the natural target images) to some extent. In this manner, the negative aspects of the synthetic images can be reduced as well. For example, although the background of generated images looks unrealistic, these fake images will be less likely to affect the classification performance because through attention alignment, the model is encouraged to pay more attention to the most discriminative parts of the object and is less likely to be drifted by the irrelevant background.

On the other hand, the EM training also benefits from the supervised data correspondence which provides labeled images in both domains. For EM training, there originally exists no constraint that the estimated hidden variable  $Z$  is assigned with the semantic meaning aligned with the ground-truth label. *i.e.* there may exist label shift or the data is clustered in an undesirable way. With more labeled data and synchronizing  $\theta^{post}$  with  $\theta$ , the above issue can be alleviated. In addition, adversarial attention alignment further regularizes the training process by encouraging the network to focus on the desirable discriminative information, which helps stabilize the training process.

## 4. Experiment

### 4.1. Datasets

We perform experiment on two domain adaptation classification datasets.

1) Digit datasets from MNIST [10] (60,000 training + 10,000 test images) to MNIST-M [5] (59,001 training + 90,001 test images). MNIST and MNIST-M are treated as the source domain and target domain, respectively. The images of MNIST-M are created by combining MNIST digits with the patches randomly extracted from color photos of BSDS500 [1] as their background.

2) Office-31 is a standard benchmark for real-world domain adaptation tasks. It consists of 4,110 images subject to 31 categories. This dataset contains three distinct domains, 1) images which are collected from the Amazon website (Amazon domain), 2) web camera (Webcam domain), and 3) digital SLR camera (DSLR domain) under different settings, respectively. The dataset is also imbalanced across domains, with 2,817 images in **A** domain, 795 images in **W** domain, and 498 images in **D** domain. We evaluate our algorithm for six transfer tasks including **A**  $\rightarrow$  **W**, **D**  $\rightarrow$  **W**, **W**  $\rightarrow$  **D**, **A**  $\rightarrow$  **D**, **D**  $\rightarrow$  **A**, and **W**  $\rightarrow$  **A** and compare our results with previous unsupervised domain adaptation methods.

### 4.2. Implementation details

**MNIST**  $\rightarrow$  **MNIST-M** The source network is trained on the MNIST training set. When the source network is trained, it is fixed to guide the training of the target network. We adopt Adam to update our network and the initial learning rate is set to 0.001. For a mini-batch input data, we fix the proportions of real source data, synthetic target data, real target data and synthetic source data as 0.35, 0.15, 0.35, and 0.15, respectively, throughout the experiment. The target and the source network are made up of four convolutional layers, where the first three are for feature extraction and the last one acts as a classifier. We align the attention between the source and target network for the three convolutional layers. For EM training, we set the threshold  $p_t = 1$  so that the network is learned with all the source and synthetic target data before the first update of  $M^{post}$ . We then set the threshold  $p_t = 0.95$  afterwards.

**Office-31** To make a fair comparison with the state-of-the-art domain adaptation methods [14], we adopt the ResNet-50 [6, 7] architecture to perform the adaptation tasks on office-31 and we start from the model pre-trained on ImageNet [4]. We first fine-tune the model on the source domain data and fix it. The source model is then used to guide the attention alignment of the target network. The target network also starts from the fine-tuned model and is gradually trained to adapt to the target domain data. We penalize the distances of the attention maps *w.r.t* all the convolutional layers except for the first convolutional and the the last max-pooling layers. We follow the same learning rate schedule adopted in [14] throughout our experiment except that we initialize the learning rate schedule after each update of posterior estimation network  $M_{post}$  (see Section 3.3). For a mini-batch input data, we fix the proportions

of real source data, synthetic target data, real target data and synthetic source data as 0.35, 0.15, 0.35, and 0.15 respectively, throughout our experiment. Threshold  $p_t$  for EM training is set as 0.95. We choose  $\beta$  through validation following the same protocol as [14].

### 4.3. Evaluation

**MNIST  $\rightarrow$  MNIST-M.** The classification results of transferring MNIST to MNIST-M are presented in Table 1. We arrive at four observations.

Method	Train Data	Accuracy (%)
CNN	S	45.6
RevGrad [5]	S + T	81.5
DSN [3]	S + T	83.2
Tri-training [19]	S + T	94.2
PixelDA [2]	S + T + T <sub>f</sub>	<b>98.2</b>
CNN	T <sub>f</sub>	75.0
CNN	S + T <sub>f</sub>	78.5
CNN + $\mathcal{L}^{AT}$	S + T <sub>f</sub>	85.7
Ours wo ( $\mathcal{L}^{AT}$ )	S + T <sub>f</sub> + T + S <sub>f</sub>	93.5
Ours w ( $\mathcal{L}^{AT}$ )	S + T <sub>f</sub> + T + S <sub>f</sub>	<b>95.6</b>

Table 1: Classification accuracy (%) for MNIST  $\rightarrow$  MNIST-M. ‘‘CNN’’ denotes the source and target network (Section 4.2). ‘‘S’’ and ‘‘T<sub>f</sub>’’ represent training the target network with source data and synthetic target data, respectively. ‘‘T’’ and ‘‘S<sub>f</sub>’’ mean training the target network with target and synthetic source data respectively.

First, our method achieves competitive performance, which outperforms the Tri-training method [19] by +1.4% (from 94.2% to 95.6%). Note that technically, PixelDA [2] is compatible to our method, and can be adopted to improve the accuracy of our model. We will investigate this in the future. Second, we observe that the accuracy of the source network drops heavily when transferred to the target domain (from 99.3% on source test set to 45.6% on target test set), which implies the significant domain shift from MNIST to MNIST-M. Third, we can see that the distribution of synthetic target data is much closer to real target data than real source data, by observing that training with synthetic target data improves the performance over the source network by about +30%. Finally, training with a mixture of source and synthetic target data is beneficial for the model to learn domain invariant features and improves the adaptation performance by +3.5% over that of the model trained with synthetic target data only.

Table 1 demonstrates that our EM training algorithm is an effective way to exploit unlabeled target domain data. Moreover, imposing the attention alignment penalty  $\mathcal{L}^{AT}$  always leads to noticeable improvement.

**Office-31.** The classification results based on ResNet-50 are shown in Table 2. With identical evaluation setting, we compare our methods with previous transfer methods and variants of our method. We have three major conclusions.

First, from Table 2, it can be seen that our method outperforms the state of art in all the transfer tasks with a large margin. The improvement is larger on harder transfer tasks, where the source domain is substantially different from and has much less data than the target domain, *e.g.* **D**  $\rightarrow$  **A**, and **W**  $\rightarrow$  **A**. Specifically, we improve over the state of art result by +2.6% on average, and by +5.1 % for the difficult transfer task **D**  $\rightarrow$  **A**.

Second, we also compare our method with and without the adversarial attention alignment loss  $\mathcal{L}^{AT}$ . Although for easy transfer tasks, the performance of these two variants are comparable, when moving to much harder tasks, we observe obvious improvement brought by the adversarial attention alignment, *e.g.*, training with adversarial attention alignment outperforms that without attention alignment by +2% for the task **D**  $\rightarrow$  **A**, and +1.7% for the task **W**  $\rightarrow$  **A**. This implies that adversarial attention alignment helps reduce the discrepancy between domains and regularize the training of the target model.

Third, we validate that augmenting with synthetic target data to facilitate the target network training brings significant improvement of accuracy over source network. This indicates that the discrepancy between synthetic and real target data is much smaller.

Fig. 4 illustrates how the attention alignment penalty  $\mathcal{L}^{AT}$  changes during the training process with and without this penalty imposed. Without attention alignment, the discrepancy of the attention maps between the source and target network is significantly larger and increases as the training goes on. The improvement of accuracy brought by adding  $\mathcal{L}^{AT}$  penalty to the objective can be attributed to the much smaller discrepancy of attention maps between the source and the target models, *i.e.*, better aligned attention mechanism. The testing accuracy curves on the target domain for tasks **D**  $\rightarrow$  **A** and **D**  $\rightarrow$  **A** are also drawn in Fig. 4. It can be seen that the test accuracy steadily increases and the model with  $\mathcal{L}^{AT}$  imposed converges much faster than that without any attention alignment.

### 4.4. Ablation study

Table 3 compares the accuracy of different EM variants. We conduct ablation studies by removing one component from the system at a time (three components are considered which are defined in Section 3.3). For each variant of EM, we also evaluate the effect of imposing  $\mathcal{L}^{AT}$  by comparing training with and without  $\mathcal{L}^{AT}$ . By comparing the performances of EM-A, EM-B, EM-C and full method we adopted, we find that the three modifications all contribute considerably to the final success. Among them, the asyn-

Method	Train Data	A $\rightarrow$ W	D $\rightarrow$ W	W $\rightarrow$ D	A $\rightarrow$ D	D $\rightarrow$ A	W $\rightarrow$ A	Average
ResNet-50	S	68.4 $\pm$ 0.2	96.7 $\pm$ 0.1	99.3 $\pm$ 0.1	68.9 $\pm$ 0.2	62.5 $\pm$ 0.3	60.7 $\pm$ 0.3	76.1
RevGrad [5]	S + T	82.0 $\pm$ 0.4	96.9 $\pm$ 0.2	99.1 $\pm$ 0.1	79.7 $\pm$ 0.4	68.2 $\pm$ 0.4	67.4 $\pm$ 0.5	82.2
JAN [14]	S + T	85.4 $\pm$ 0.3	97.4 $\pm$ 0.2	99.8 $\pm$ 0.2	84.7 $\pm$ 0.3	68.6 $\pm$ 0.3	70.0 $\pm$ 0.4	84.3
JAN-A [14]	S + T	86.0 $\pm$ 0.4	96.7 $\pm$ 0.3	99.7 $\pm$ 0.1	85.1 $\pm$ 0.4	69.2 $\pm$ 0.4	70.7 $\pm$ 0.5	84.6
ResNet-50	T <sub>f</sub>	81.1 $\pm$ 0.2	98.5 $\pm$ 0.2	99.8 $\pm$ 0.0	83.3 $\pm$ 0.3	61.0 $\pm$ 0.2	60.2 $\pm$ 0.3	80.6
ResNet-50	S + T <sub>f</sub>	81.9 $\pm$ 0.2	98.5 $\pm$ 0.2	99.8 $\pm$ 0.0	83.7 $\pm$ 0.3	66.5 $\pm$ 0.2	64.8 $\pm$ 0.3	82.5
Ours (wo $\mathcal{L}^{AT}$ )	S + T <sub>f</sub> + T + S <sub>f</sub>	<b>87.1</b> $\pm$ 0.3	<b>99.3</b> $\pm$ 0.1	<b>100</b> $\pm$ 0.0	87.1 $\pm$ 0.2	72.3 $\pm$ 0.2	72.2 $\pm$ 0.2	86.3
Ours (w $\mathcal{L}^{AT}$ )	S + T <sub>f</sub> + T + S <sub>f</sub>	86.8 $\pm$ 0.2	<b>99.3</b> $\pm$ 0.1	<b>100</b> $\pm$ 0.0	<b>88.8</b> $\pm$ 0.4	<b>74.3</b> $\pm$ 0.2	<b>73.9</b> $\pm$ 0.2	<b>87.2</b>

Table 2: Classification accuracy (%) on the Office-31 dataset compared with the state-of-the-art methods based on ResNet-50.

Method	Train Data	A $\rightarrow$ W	A $\rightarrow$ D	D $\rightarrow$ A	W $\rightarrow$ A	Average
ResNet-50	S	68.4 $\pm$ 0.2	68.9 $\pm$ 0.2	62.5 $\pm$ 0.3	60.7 $\pm$ 0.3	65.1
EM-A	S + T <sub>f</sub> + T + S <sub>f</sub>	68.6 $\pm$ 0.3	73.5 $\pm$ 0.3	62.7 $\pm$ 0.3	52.8 $\pm$ 0.3	64.4
EM-A + $\mathcal{L}^{AT}$	S + T <sub>f</sub> + T + S <sub>f</sub>	80.4 $\pm$ 0.2	79.1 $\pm$ 0.2	66.4 $\pm$ 0.2	58.4 $\pm$ 0.2	71.1
EM-C	S + T <sub>f</sub> + T + S <sub>f</sub>	86.4 $\pm$ 0.3	87.0 $\pm$ 0.3	69.5 $\pm$ 0.3	71.4 $\pm$ 0.3	78.6
EM-C + $\mathcal{L}^{AT}$	S + T <sub>f</sub> + T + S <sub>f</sub>	86.2 $\pm$ 0.2	86.6 $\pm$ 0.3	71.8 $\pm$ 0.3	73.7 $\pm$ 0.2	79.6
EM-B	S + T <sub>f</sub> + T + S <sub>f</sub>	<i>very low</i>	<i>very low</i>	<i>very low</i>	<i>very low</i>	<i>very low</i>
EM-B + $\mathcal{L}^{AT}$	S + T <sub>f</sub> + T + S <sub>f</sub>	<i>very low</i>	<i>very low</i>	<i>very low</i>	<i>very low</i>	<i>very low</i>
Ours (wo $\mathcal{L}^{AT}$ )	S + T <sub>f</sub> + T + S <sub>f</sub>	<b>87.1</b> $\pm$ 0.3	87.1 $\pm$ 0.2	72.3 $\pm$ 0.2	72.2 $\pm$ 0.2	79.7
Ours (w $\mathcal{L}^{AT}$ )	S + T <sub>f</sub> + T + S <sub>f</sub>	86.8 $\pm$ 0.2	<b>88.8</b> $\pm$ 0.4	<b>74.3</b> $\pm$ 0.2	<b>73.9</b> $\pm$ 0.2	<b>80.9</b>

Table 3: Variants of the EM algorithm with and without  $\mathcal{L}^{AT}$ . The EM algorithm without asynchronous update of  $M^{post}$  is denoted by EM-A, while that without filtering the noisy data using threshold  $p_t$  is denoted by EM-B. EM-C represents EM training without initializing the learning rate schedule when  $M^{post}$  is updated.

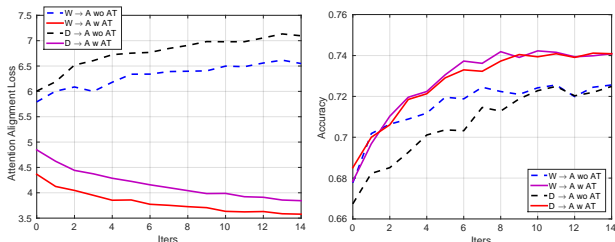


Figure 4: Analysis of the training process (EM is implemented). **Left:** The trend of  $\mathcal{L}^{AT}$  during training with and without imposing the  $\mathcal{L}^{AT}$  penalty term. **Right:** The curves of test accuracy on the target domain. The results of tasks **W**  $\rightarrow$  **A** and **D**  $\rightarrow$  **A** are presented. The results for other tasks are similar. One iteration here represents one update of the network  $M^{post}$  (see Section 3.3).

chronous update is the most important factor.

We also notice that for EM-A and EM-C, training along with  $\mathcal{L}^{AT}$  always leads to a significant improvement, implying performing attention alignment is an effective way to improve the adaptation performance.

#### 4.5. Attention alignment criteria comparison

As discussed in section 3.2, after normalizing the attention maps across paired samples, the  $L_2$ -norm is applied to measure the distance between them, where  $L_1$ -norm can be an alternative choice. Also, MMD or JMMD can be technically adopted to measure the discrepancy of attentions across domains. We compare these criteria for performing

Criterion	<b>D</b> $\rightarrow$ <b>A</b>	<b>W</b> $\rightarrow$ <b>A</b>
$L_1$ -norm	<i>very low</i>	<i>very low</i>
MMD	66.2	64.5
JMMD	67.4	66.3
Ours	74.3	73.9

Table 4: Comparison for different attention alignment criteria. The classification accuracies are shown for tasks **D**  $\rightarrow$  **A** and **W**  $\rightarrow$  **A** on Office-31.

attention alignment in Table 4. We find that our method achieves the best results among all these criteria. The  $L_1$ -norm fails to train a workable network because it is misled

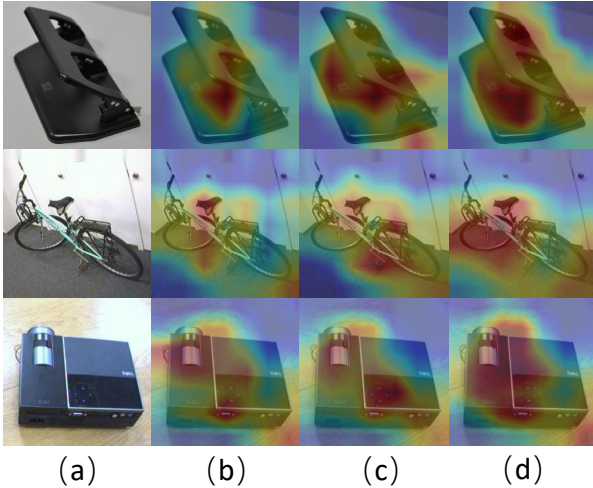


Figure 5: Visualization of attention maps. (a): The original target input image. (b): The source network. (c): The target network (trained on labeled target data). (d): The target network trained with adversarial attention alignment. We observe that performing attention alignment between the target and the source network largely improves the attention mechanism on the target domain data. Notably, the attention mechanism of the target network trained using adversarial attention alignment is even better than that trained on its own domain labeled data, *i.e.*, (d) is better than (c).

by the noise existing in the attention maps. Our method outperforms MMD or JMMD by a large margin, mainly due to the structure reservation, as discussed in section 3.2.

#### 4.6. Visualization

The aim of attention alignment is to enable the target network to attend to the discriminative parts of an image before making predictions. Fig. 4 has shown that imposing attention alignment penalty effectively reduces the distance of the attention maps between the target network and the source network which is trained on labeled source data and has a well-aligned attention mechanism.

In Fig. 5, we visualize the attention maps for the same target image, obtained by passing the image through a source network, a target network trained on labeled target data, and a target network trained by adversarial attention alignment without using any target label information. It demonstrates that through attention alignment, the attention of the target network can be well adapted to the target domain data, and is even better than the one obtained through its own domain labeled data.

## 5. Conclusion

In this paper, we make two contributions to the community of unsupervised domain adaptation. First, from the *convolutional layers*, we propose to align the attention maps of the source network and target network. Through minimizing the discrepancy of attention mechanisms across domains, the knowledge from source network can be better adapted to the target network. Second, from an *EM perspective*, we maximize the likelihood of unlabeled target data. Along with minimizing the cross-entropy loss for the labeled source data, the EM algorithm allows us to leverage more training data for better domain adaptation. Both contributions benefit from the unsupervised image correspondences provided by CycleGAN. Experiment demonstrates that the two contributions both have positive effects on the system performance. On two benchmark datasets, we achieve the state-of-the-art results compared to the previous domain adaptation methods.

## References

- [1] Pablo Arbelaez, Michael Maire, Charless Fowlkes, and Jitendra Malik. Contour detection and hierarchical image segmentation. *IEEE transactions on pattern analysis and machine intelligence*, 33(5):898–916, 2011. 6
- [2] Konstantinos Bousmalis, Nathan Silberman, David Dohan, Dumitru Erhan, and Dilip Krishnan. Unsupervised pixel-level domain adaptation with generative adversarial networks. *arXiv preprint arXiv:1612.05424*, 2016. 3, 7
- [3] Konstantinos Bousmalis, George Trigeorgis, Nathan Silberman, Dilip Krishnan, and Dumitru Erhan. Domain separation networks. In *Advances in Neural Information Processing Systems*, pages 343–351, 2016. 7
- [4] Jia Deng, Wei Dong, Richard Socher, Li-Jia Li, Kai Li, and Li Fei-Fei. Imagenet: A large-scale hierarchical image database. In *Computer Vision and Pattern Recognition, 2009. CVPR 2009. IEEE Conference on*, pages 248–255. IEEE, 2009. 6
- [5] Yaroslav Ganin and Victor Lempitsky. Unsupervised domain adaptation by backpropagation. In *International Conference on Machine Learning*, pages 1180–1189, 2015. 2, 6, 7, 8
- [6] Kaiming He, Xiangyu Zhang, Shaoqing Ren, and Jian Sun. Deep residual learning for image recognition. In *Proceedings of the IEEE conference on computer vision and pattern recognition*, pages 770–778, 2016. 6

- [7] Kaiming He, Xiangyu Zhang, Shaoqing Ren, and Jian Sun. Identity mappings in deep residual networks. In *European Conference on Computer Vision*, pages 630–645. Springer, 2016. 6
- [8] Judy Hoffman, Eric Tzeng, Taesung Park, Jun-Yan Zhu, Phillip Isola, Kate Saenko, Alexei A Efros, and Trevor Darrell. Cycada: Cycle-consistent adversarial domain adaptation. *arXiv preprint arXiv:1711.03213*, 2017. 3
- [9] Taeksoo Kim, Moonsu Cha, Hyunsoo Kim, Jungkwon Lee, and Jiwon Kim. Learning to discover cross-domain relations with generative adversarial networks. *arXiv preprint arXiv:1703.05192*, 2017. 3
- [10] Yann LeCun, Léon Bottou, Yoshua Bengio, and Patrick Haffner. Gradient-based learning applied to document recognition. *Proceedings of the IEEE*, 86(11):2278–2324, 1998. 6
- [11] Ming-Yu Liu, Thomas Breuel, and Jan Kautz. Unsupervised image-to-image translation networks. *arXiv preprint arXiv:1703.00848*, 2017. 3
- [12] Ming-Yu Liu and Oncel Tuzel. Coupled generative adversarial networks. In *Advances in neural information processing systems*, pages 469–477, 2016. 3
- [13] Mingsheng Long, Yue Cao, Jianmin Wang, and Michael Jordan. Learning transferable features with deep adaptation networks. In *International Conference on Machine Learning*, pages 97–105, 2015. 2, 5
- [14] Mingsheng Long, Jianmin Wang, and Michael I Jordan. Deep transfer learning with joint adaptation networks. *arXiv preprint arXiv:1605.06636*, 2016. 2, 5, 6, 7, 8
- [15] Artem Rozantsev, Vincent Lepetit, and Pascal Fua. On rendering synthetic images for training an object detector. *Computer Vision and Image Understanding*, 137:24–37, 2015. 3
- [16] Artem Rozantsev, Mathieu Salzmann, and Pascal Fua. Beyond sharing weights for deep domain adaptation. *arXiv preprint arXiv:1603.06432*, 2016. 2
- [17] Artem Rozantsev, Mathieu Salzmann, and Pascal Fua. Residual parameter transfer for deep domain adaptation. *arXiv preprint arXiv:1711.07714*, 2017. 2
- [18] Paolo Russo, Fabio Maria Carlucci, Tatiana Tommasi, and Barbara Caputo. From source to target and back: symmetric bi-directional adaptive gan. *arXiv preprint arXiv:1705.08824*, 2017. 3
- [19] Kuniaki Saito, Yoshitaka Ushiku, and Tatsuya Harada. Asymmetric tri-training for unsupervised domain adaptation. *arXiv preprint arXiv:1702.08400*, 2017. 7
- [20] Ramprasaath R Selvaraju, Abhishek Das, Ramakrishna Vedantam, Michael Cogswell, Devi Parikh, and Dhruv Batra. Grad-cam: Why did you say that? visual explanations from deep networks via gradient-based localization. *arXiv preprint arXiv:1610.02391*, 2016. 1, 2
- [21] Ashish Shrivastava, Tomas Pfister, Oncel Tuzel, Josh Susskind, Wenda Wang, and Russ Webb. Learning from simulated and unsupervised images through adversarial training. *arXiv preprint arXiv:1612.07828*, 2016. 3
- [22] Karen Simonyan, Andrea Vedaldi, and Andrew Zisserman. Deep inside convolutional networks: Visualising image classification models and saliency maps. *arXiv preprint arXiv:1312.6034*, 2013. 1, 2
- [23] Baochen Sun and Kate Saenko. Deep coral: Correlation alignment for deep domain adaptation. In *Computer Vision–ECCV 2016 Workshops*, pages 443–450. Springer, 2016. 2
- [24] Eric Tzeng, Judy Hoffman, Trevor Darrell, and Kate Saenko. Simultaneous deep transfer across domains and tasks. In *Proceedings of the IEEE International Conference on Computer Vision*, pages 4068–4076, 2015. 2
- [25] Eric Tzeng, Judy Hoffman, Kate Saenko, and Trevor Darrell. Adversarial discriminative domain adaptation. *arXiv preprint arXiv:1702.05464*, 2017. 2
- [26] Eric Tzeng, Judy Hoffman, Ning Zhang, Kate Saenko, and Trevor Darrell. Deep domain confusion: Maximizing for domain invariance. *arXiv preprint arXiv:1412.3474*, 2014. 2
- [27] Sergey Zagoruyko and Nikos Komodakis. Paying more attention to attention: Improving the performance of convolutional neural networks via attention transfer. *arXiv preprint arXiv:1612.03928*, 2016. 1, 3, 4
- [28] Matthew D Zeiler and Rob Fergus. Visualizing and understanding convolutional networks. In *European conference on computer vision*, pages 818–833. Springer, 2014. 1, 2
- [29] Zhedong Zheng, Liang Zheng, and Yi Yang. Unlabeled samples generated by gan improve the person re-identification baseline in vitro. *arXiv preprint arXiv:1701.07717*, 3, 2017. 3

- [30] Bolei Zhou, Aditya Khosla, Agata Lapedriza, Aude Oliva, and Antonio Torralba. Learning deep features for discriminative localization. In *Proceedings of the IEEE Conference on Computer Vision and Pattern Recognition*, pages 2921–2929, 2016. [1](#), [2](#)
- [31] Jun-Yan Zhu, Taesung Park, Phillip Isola, and Alexei A Efros. Unpaired image-to-image translation using cycle-consistent adversarial networks. *arXiv preprint arXiv:1703.10593*, 2017. [2](#), [3](#)